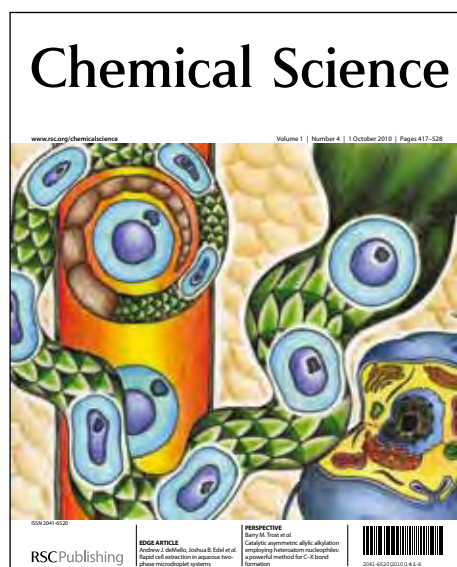


Chemical Science

Accepted Manuscript



This is an *Accepted Manuscript*, which has been through the RSC Publishing peer review process and has been accepted for publication.

Accepted Manuscripts are published online shortly after acceptance, which is prior to technical editing, formatting and proof reading. This free service from RSC Publishing allows authors to make their results available to the community, in citable form, before publication of the edited article. This *Accepted Manuscript* will be replaced by the edited and formatted *Advance Article* as soon as this is available.

To cite this manuscript please use its permanent Digital Object Identifier (DOI®), which is identical for all formats of publication.

More information about *Accepted Manuscripts* can be found in the [Information for Authors](#).

Please note that technical editing may introduce minor changes to the text and/or graphics contained in the manuscript submitted by the author(s) which may alter content, and that the standard [Terms & Conditions](#) and the [ethical guidelines](#) that apply to the journal are still applicable. In no event shall the RSC be held responsible for any errors or omissions in these *Accepted Manuscript* manuscripts or any consequences arising from the use of any information contained in them.

EDGE ARTICLE

Fluorophore Incorporation Allows Nanomolar Guest Sensing and White-Light Emission in M_4L_6 Cage Complexes[†]

Cite this: DOI: 10.1039/x0xx00000x

Prakash P. Neelakandan,^a Azucena Jiménez,^a and Jonathan R. Nitschke^{a*}

Received 00th January 2012,

Accepted 00th January 2012

DOI: 10.1039/x0xx00000x

www.rsc.org/

We have prepared a series of M_4L_6 tetrahedral cages containing BODIPY and pyrene moieties and followed their guest-binding properties through electronic absorption and fluorescence spectroscopies. Our results indicate that these cages are capable of encapsulating anions, leading to colour and fluorescence changes; the use of fluorescence spectroscopy thus allowed for guest detection at nanomolar concentration. On the basis of our observations, we developed an inexpensive test-paper strip assay for easy and practical detection of anions. These cages were also found to encapsulate polycyclic aromatic hydrocarbons such as perylene. By manipulating the concentration of host and guest species, we developed a white-light-emitting ensemble. Additionally, these metal-organic cages were observed to react with amino acids, allowing the sensing of these analytes. These multi-functional cages' interactions with light thus enable new applications.

Introduction

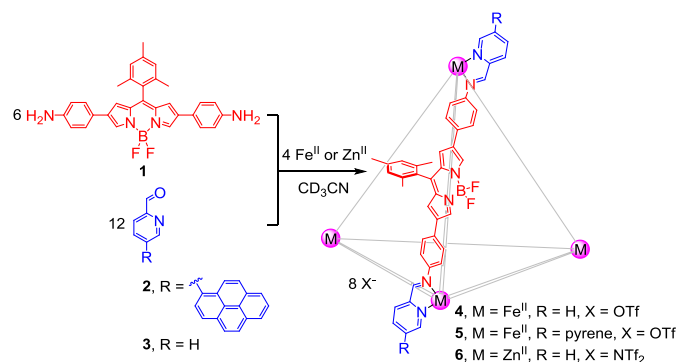
Recent research on complex supramolecules has been driven not only by interest in the design of increasingly complex forms, but also by their wide-ranging applications.¹⁻¹⁰ Among supramolecules, metal-organic assemblies have gained particular attention. They can be synthesized easily through designed coordinative interactions involving preformed ligands,¹¹⁻¹⁷ or through subcomponent self-assembly in which the ligands are prepared *in situ* from precursors.¹⁸⁻²¹ Moreover, an appropriate selection of building blocks allows properties to be tailored for diverse applications.²² Hollows may thus be incorporated, allowing for the exploration of host-guest functionality. Recent examples include the stabilization of reactive species,^{23, 24} catalysis,²⁵⁻²⁷ photoreactions,²⁸⁻³⁰ and selective recognition of substrates.³¹⁻³⁶

Even though metal-organic capsules are known to encapsulate and stabilize guest molecules within their cavities, their utility as molecular sensors has only begun to be explored.³⁷⁻⁴³ This is partly because NMR spectroscopy is used in the majority of cases for analysing host-guest binding. Although NMR spectroscopy is one of the most versatile experimental techniques for interpreting molecular interactions, it is less sensitive than other techniques.⁴⁴ Optical spectroscopies, such as electronic absorption and fluorescence, have inherently higher sensitivity than NMR and are widely utilized for studying host-guest interactions.⁴⁵⁻⁴⁷ Therefore, we reasoned that a metal-organic capsule incorporating

fluorophores would provide an ideal platform to study guest encapsulation at lower concentrations, thereby allowing the sensitivity limits of molecular recognition in these systems to be probed. In addition, the subcomponent self-assembly method would enable incorporation of multiple chromophores site-selectively.

Herein, we describe the synthesis of a series of fluorescent metallo-supramolecular capsules containing 4,4-difluoro-4-bora-3a,4a-diaza-*s*-indacene (BODIPY) and pyrene residues. These fluorophores were selected on the basis of their useful photophysical properties and established optoelectronic applications.⁴⁸⁻⁵⁰ BODIPY and pyrene moieties were incorporated into amine and aldehyde building blocks **1** and **2**, respectively, which then underwent subcomponent self-assembly involving the simultaneous formation of both dynamic covalent (C=N) and coordinative (L→M) bonds to yield metal-organic cages **4-6** (Scheme 1). We observed significant changes in the optical properties of both chromophores upon cage formation. Subsequent investigations of guest binding indicate that these cages are able to detect nanomolar concentrations of anionic substrates. On the basis of our observations, we developed a test-paper strip assay for the straightforward visual recognition of anions. Furthermore, we discovered that the cage **5** interacts with perylene, thereby leading to a white-light-emitting ensemble. Finally, these cages have been employed for the optical sensing of amino acids, which takes advantage of the dynamic nature of bonds between subcomponents. This process proceeds through the analyte-

induced rupture of the cages. Our results demonstrate that cage frameworks synthesized from a set of simple building blocks can perform multiple functions and thus highlight the utility of subcomponent self-assembly in constructing functional materials.

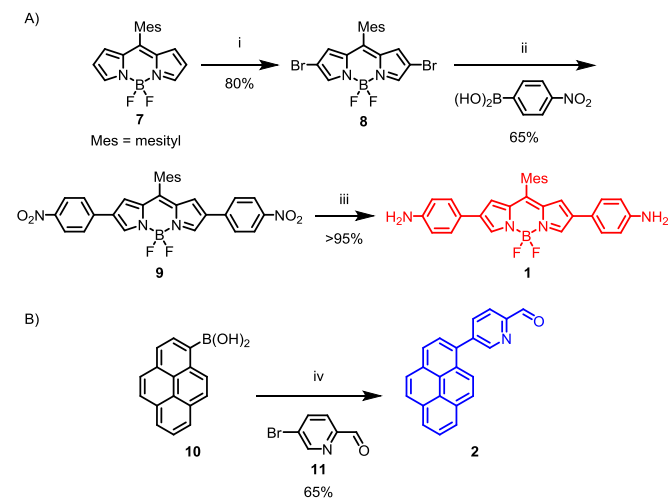


Scheme 1. Subcomponent self-assembly of the bis(aminophenyl)BODIPY **1** to form M₄L₆ cages. The structure of only one edge is shown for clarity.

RESULTS AND DISCUSSION

Subcomponent Syntheses and Cage Preparation

The syntheses of subcomponents **1** and **2** were accomplished as shown in Scheme 2. Following a reported procedure, 8-mesityl BODIPY (**7**)⁵¹ was brominated using *N*-bromosuccinimide (NBS) to yield dibromo derivative **8**, which subsequently underwent coupling with 4-nitrophenylboronic acid under Suzuki-Miyaura conditions to yield bis(nitrophenyl) BODIPY **9**.⁵² The linear bis(aminophenyl) BODIPY **1** was obtained by reducing the bis(nitrophenyl) BODIPY derivative **9** using dihydrogen in the presence of Pd/C as catalyst. Similarly, commercially available pyrene-1-boronic acid (**10**) and 5-bromo-2-formylpyridine (**11**) were joined *via* Suzuki-Miyaura cross-coupling to yield pyrene-appended formylpyridine (**2**) in 65 % yield.



Scheme 2. Syntheses of (A) bis(aminophenyl)BODIPY **1** and (B) pyrene-appended formylpyridine **2**. Reaction conditions: (i) NBS, 1 : 1 DCM : DMF, 25 °C, 8 h, 80 %;

(ii) 4-nitrophenylboronic acid, Pd₂(dba)₃·CHCl₃, ^tBu₃P·HBF₄, Cs₂CO₃, THF : water, 25 °C, 24 h, 65 %; (iii) H₂/Pd-C, methanol, 25 °C, 5 h, 95 %; (iv) Pd(PPh₃)₄, aq. NaOH (1 M), toluene, 100 °C, 30 min, 200 W microwave, 65 %.

UV-Vis absorption and fluorescence spectra of the subcomponents **1** and **2** are presented in Fig. S1. Bis(aminophenyl)BODIPY **1** exhibited an intense green colour and the absorption peak corresponding to its S₀ → S₁ transition was broad and bathochromically shifted (λ_{max} = 655 nm), whereas its fluorescence was completely quenched. This behaviour contrasts with the commonly-observed sharp absorption and emission spectra for most BODIPY derivatives.^{48, 50} However, both the absorption and fluorescence properties of **1** were comparable to a previously reported bis(*N,N*-dimethylaminophenyl)BODIPY derivative⁵² and could be explained by invoking an intramolecular charge transfer (ICT) state involving the aminophenyl units and the BODIPY core in **1**.^{52, 53}

The optical spectroscopic features of the pyrene appended 2-formylpyridine (**2**) were also unusual. In comparison to the parent fluorophore pyrene, the UV-Vis absorption spectrum of **2** lacked the characteristic vibrational structure; a plateau was instead observed in the region from 340 to 355 nm in acetonitrile. Similarly, the fluorescence spectrum of **2** was broad with an emission maximum at 525 nm and lacked the characteristic vibrational structure. The fluorescence quantum yield (Φ_F) of **2** was found to be 0.16. In order to understand the optical properties of **2**, we investigated the effects of solvent polarity and temperature (Fig. S2 and S3). We observed a bathochromic shift in the emission maximum of **2** with an increase in solvent polarity. Similarly, the emission maximum of **2** was found to vary at different temperatures – we observed an emission maximum of 530 nm at 10 °C which underwent a hypsochromic shift on increasing the temperature to 513 nm at 80 °C. However, both the solvent polarity and temperature had negligible effects on the excitation spectra of **2**. On the basis of these observations and previous reports,⁵⁴ we assign the broad red-shifted emission in **2** to an intramolecular exciplex-type state.

Scheme 1 depicts the subcomponent self-assembly of bis(aminophenyl)BODIPY **1** with 2-formylpyridines **2** and **3** and the metal ions Fe^{II} and Zn^{II}. The reaction between **1** and 2-formylpyridine (**3**) together with iron(II) trifluoromethanesulfonate (triflate, -OTf) or zinc(II) di[bis(trifluoromethylsulfonyl) imide] (triflimide, -NTf₂) in acetonitrile yielded cages **4** and **6**, respectively, as the exclusively-observed products. Similarly, the reaction of **1** with pyrene-appended formylpyridine (**2**) and Fe(OTf)₂ afforded the corresponding cage **5**. The identities of these M₄L₆ cages were established by one- and two-dimensional NMR and mass spectrometry (Fig. 1, S4-S9). ¹H and ¹⁹F NMR spectra of **4-6** were consistent with complex mixtures of diastereomeric products having Λ and Δ configurations at the metal stereocenters, as has been previously observed.^{18, 55-57}

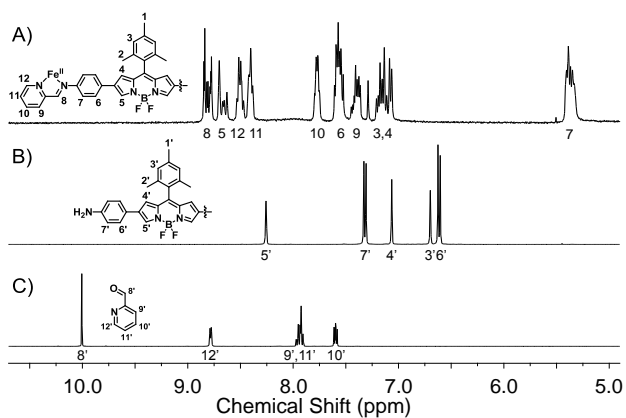


Fig. 1. Partial ^1H NMR spectra of (A) cage **4** and the subcomponents (B) **1** and (C) **3** in CD_3CN .

In order to visualize the cages' geometries, we employed molecular modelling.⁵⁸ The energy-optimized structures of **4-6** (Fig. 2) were analogous to those of previously reported M_4L_6 cages.¹⁸ Models indicated that the mesityl groups of the BODIPY moieties could point into the cavities, out of them, or in any direction in between these two extremes, which we infer to add additional complexity to the observed NMR spectra. Possibly due to this stereochemical diversity in solution, our efforts aimed at growing single crystals of the cages were unsuccessful.

Metal-ion-mediated self-assembly brought about changes to the optical properties of the BODIPY chromophore. As compared to subcomponent **1**, cages **4-6** exhibited sharper $S_0 \rightarrow S_1$ transitions and the absorption maxima were shifted into the shorter wavelength region ($\Delta\lambda = 70$ to 100 nm, Fig. S1). Moreover, the fluorescence of the BODIPY moiety was "turned-on" during self-assembly and the quantum yields of fluorescence were found to be $\Phi_F = 0.012$, 0.015 and 0.055 for **4-6**, respectively. Cage formation also influenced the absorption and fluorescence properties of the pyrene moiety in **2**. We observed a blue shift of *ca.* 10 nm in its absorption maximum whereas a new shoulder was observed in the fluorescence spectrum around 400 nm. Moreover, the fluorescence quantum yield of cage **5** was significantly diminished (*ca.* 10 -fold) as compared to that of the subcomponent **2**. The changes in the optical properties of the

subcomponents upon cage formation could be attributed to the disruption of ICT/exciple states during imine formation.

Interaction with Anions

The favourable optical properties of metallo-supramolecular cages **4-6** led us to investigate their interaction with a variety of prospective guests. As shown in Fig. 3A, the titration of tetrabutylammonium acetate into a solution of **4** in acetonitrile resulted in a gradual decrease in the absorbance at 555 nm with a concomitant increase in longer-wavelength absorption. Isosbestic points were observed at 588 , 464 , 268 and 252 nm. When the concentration of acetate exceeded that of the cage, we observed a shift in the absorption maximum from 555 to 606 nm. In the emission spectrum, the addition of acetate resulted in a regular increase in the fluorescence intensity at 653 nm. In the presence of excess acetate, we observed a *ca.* 25 -fold increase in the fluorescence intensity along with a bathochromic shift of ~ 5 nm (Fig. 3B). The changes in both the absorption (bathochromic shift) and fluorescence (enhancement in intensity) enabled visual dual-mode recognition of acetate (insets of Fig. 3A and 3B). Importantly, these optical changes were sufficient to allow the detection of nanomolar concentrations of acetate.

Subsequently, titrations were carried out with other anions to investigate if cage **4** exhibited selectivity towards other anions. As shown in Fig. 1C, acetate and azide induced significant enhancements in the fluorescence of **4**, whereas moderate responses were obtained with fluoride and chloride. However, only negligible changes were observed in the fluorescence of **4** upon the addition of bromide, iodide, nitrate, hexafluorophosphate, triflate, perchlorate and tetrafluoroborate. The observed anion binding affinities of **4** could be attributed to the relative nucleophilicity and hydrogen-bond acceptor strength of the guests.⁵⁹ To gain insight into the interaction between **4** and anions, we carried out NMR titrations of **4** with acetate and azide. Although the ^1H NMR spectrum of **4** exhibited negligible changes in the presence of these anions (Fig. S10) we observed deviations in the chemical shifts of the fluorine atoms of the BODIPY groups in its ^{19}F NMR spectrum (Fig. S11), thereby confirming the interaction of the cage with acetate.

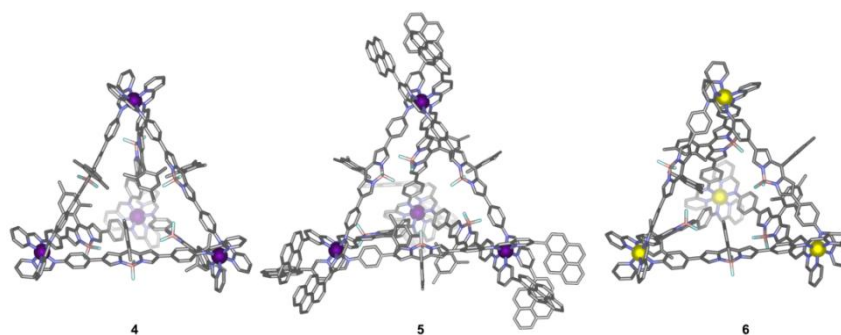


Fig. 2. Energy minimized structures of cages **4-6** obtained at the MM2 level using CAChe Workspace.

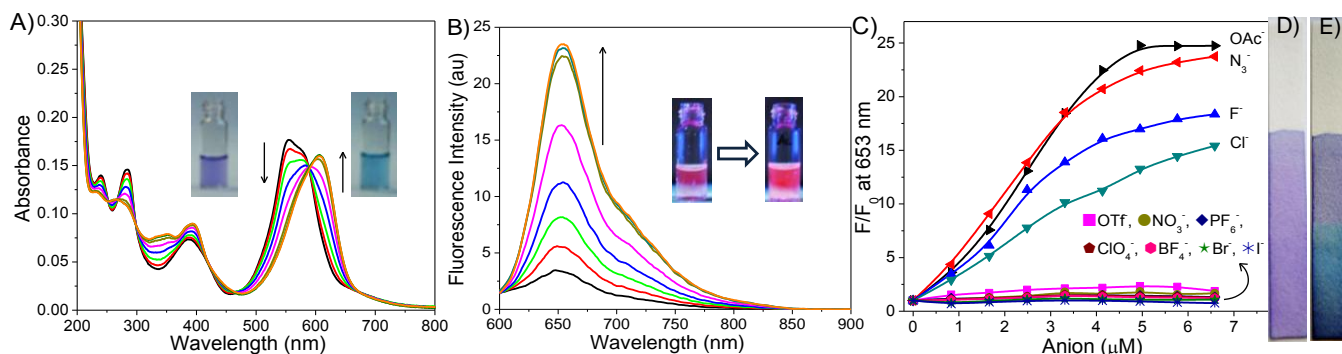


Fig. 3. Changes in the (A) UV-Vis absorption and (B) fluorescence spectra ($\lambda_{\text{ex}} = 590 \text{ nm}$) of **4** (67 nM) with the addition of tetrabutylammonium acetate (0–5.77 μM) in acetonitrile. Insets of (A) and (B) show photographs of **4** (67 nM) in acetonitrile in the absence and presence of acetate (5.77 μM). (C) Relative changes in the fluorescence intensity of **4** (67 nM) at 653 nm in the presence of selected anions. (D) Photographs of a filter paper test-strip coated with **4** and (E) the same strip after dipping the bottom half in an aqueous solution of sodium azide (1 mM).

Taking advantage of the clear changes in the optical spectra of **4** in the presence of anions, we devised a test-paper strip test for the visual detection of anions. The strip was prepared by dip-coating an acetonitrile solution of **4** onto commercially available Whatman filter paper. Upon exposure to a 1 mM aqueous solution of strongly interacting anions such as acetate, azide, fluoride or chloride, the strip changed colour from purple to greenish-blue (Fig. 3D and 3E). Thus, this test-paper strip assay serves as a rapid and straightforward technique for the qualitative detection of certain anions in aqueous media.⁶⁰

In order to compare the guest binding capabilities of **4** with those of related cages, we carried out optical titrations of **5** and **6** with anions. Cages **5** and **6** have tetrahedral molecular geometries analogous to that of **4** and are expected to behave similarly to **4**. As anticipated, the addition of acetate to an acetonitrile solution of **5** resulted in a significant bathochromic shift in its absorption maximum (Fig. S12). Similarly, the fluorescence response of pyrene-containing **5** towards acetate was comparable to that of **4**. As shown in Fig. S12, we observed that the addition of excess acetate resulted in 28-fold enhancement in fluorescence intensity at 653 nm when excited at 590 nm (corresponding to the absorption maximum of the BODIPY moiety). However, under identical conditions, we observed negligible changes in the fluorescence intensity of the pyrene moiety of **5** when excited at 333 nm (inset of Fig. S12).

We then investigated the interaction between Zn^{II} cage **6** and selected anions. The addition of acetate to a solution of **6** in acetonitrile resulted in a significant bathochromic shift in the absorption maximum from 559 to 606 nm (Fig. S13), which is comparable to the changes observed with **4** and **5**. However, the fluorescence response of **6** differed significantly from those of **4** and **5**; we observed negligibly small enhancement in the fluorescence intensity of **6** upon the addition of acetate (Fig. S14–S15). As the fluorescence quantum yield of **6** is inherently higher than that of **4**, acetate appears not to further enhance this fluorescence through binding. We have also investigated the interaction of the subcomponent **1** with anions. In contrast to the observations with cages **4–6**, addition of acetate to **1** resulted in minor changes in its absorbance (Fig. S16).

The presence of six BODIPY moieties in the cage architecture increased the molar absorptivity of the cages as compared to single-fluorophore systems. This enabled us to use dilute solutions of the cages for optical titrations. In order to understand if the cages were stable at these low concentrations, we monitored time-dependent changes in the optical spectra of cage **4** alone and also in the presence of the metal ion-chelating agent disodium ethylenediaminetetraacetic acid (EDTA). As shown in Fig. S17, the absorption maximum of **4** shifted to 607 nm in the presence of EDTA which indicates the de-coordination of the BODIPY-imines from the metal centre. In contrast, the optical spectra remained unperturbed in the absence of EDTA thereby indicating the presence of a stable cage at nanomolar concentrations.

The following three observations are relevant in understanding the interaction between cages and anions: First, changes observed in the absorption spectra of cages **4–6** following the addition of acetate were similar and the same absorption maxima were observed for **4–6** in the presence of excess acetate (Fig. S13). This indicates that all three cages interact with guests in a similar fashion. Second, subcomponent **1** was not observed to interact with anions (Fig. S16), thereby highlighting the importance of positive charges as well as the three-dimensional cavities of cages for anion recognition. Third, the absorption spectrum of cage **4** in the presence of acetate resembles that of **4** in the presence of EDTA (Fig. S13 and S17). Hence, it is plausible that addition of anions could lead to partial de-coordination of the ligands. However, the enhancement in the fluorescence of cage **4** in the presence of anions was significantly higher than was induced by EDTA (Fig. 3B and Fig. S17), which suggests that anions interact strongly with cages rather than merely de-coordinating the ligands. Finally, even in the presence of large excess of anions, we did not observe the red-shifted absorption spectrum characteristic of the subcomponent **1** ($\lambda_{\text{max}} = 655 \text{ nm}$). This led us to infer that the cages remain intact after binding anions. On the basis of the above observations we hypothesize that the cage structure was essential for anion recognition. We attribute electrostatic and anion- π interactions to be the driving forces

behind the recognition event.⁶¹⁻⁶⁷ The observed red-shift in the absorption spectra of **4-6** in the presence of anions could be attributed to the perturbation of the ligands' π orbitals due to anion- π interactions.

Cage **5** contains two types of fluorophores, arranged both along the edges and at the vertices of the cage. The binding of a guest within the cavity of the cage is expected to induce selective changes in the optical properties of the chromophores along the edges rather than those outside the vertices. In keeping with this inference, we observed significant enhancement in the fluorescence of BODIPY, whereas the pyrene fluorescence remained unperturbed (Fig. S12). This observation, together with the perturbation of the ¹⁹F NMR signals of the BF₂ groups (Fig. S11), suggests that anions could be bound within the cage cavity, which is a commonly observed binding mode for this class of molecules.^{18, 24, 59}

White-Light-Emitting Ensemble

As presented above, by following the subcomponent self-assembly pathway, we have effortlessly synthesized supramolecular metal-organic cages from simple building blocks and have incorporated multiple chromophores in a single cage framework. Moreover, our preliminary results indicate that minor modifications in the cage structure (*eg.* identity of M^{II} or guest binding) result in significant variations in their fluorescence properties. Therefore, these systems could be envisaged to have photophysical applications and may be considered as complementary to multi-chromophoric systems whose syntheses involve multi-step organic transformations.^{68, 69} In this context, we set out to fine-tune the fluorescence output from these cages as a function of guest binding. With this objective, we carried out optical titrations of cage **5** with the polycyclic aromatic hydrocarbon (PAH) perylene. The addition of perylene to a solution of **5** in acetonitrile resulted in hypochromicity of the absorption at 555 nm (Fig. S18). In contrast, the absorbance corresponding to the pyrene moiety in the region between 340-355 nm remained unaffected. During fluorescence titrations, when **5** was excited at 590 nm (where the excitation energy was exclusively absorbed by the BODIPY chromophore), we observed an enhancement in fluorescence intensity. When an excitation wavelength of 333 nm was used (absorbed by both pyrene and BODIPY fluorophores), the fluorescence from the pyrene moiety at 525 nm remained intact whereas the BODIPY fluorescence exhibited an enhancement in intensity. Titrations carried out with naphthalene, anthracene and pyrene suggest that **5** exhibits similar low binding affinity towards these other PAHs without significant selectivity (Fig. S19).

Titration of perylene into cage **5** provided the following observations: Initial aliquots of perylene increased both red and blue emission, but once the cage cavity had been filled, only blue emission was enhanced upon further additions of perylene (Fig. S18), allowing the colour of emission to be tuned. Thus, as shown in Fig. 4, the fluorescence from a mixture of **5** and perylene in 1:3 ratios had equivalent intensities in the blue, green and red regions of the electromagnetic spectrum. This

emission spectrum was broad and covered the entire visible region leading to white light emission with a fluorescence quantum yield of $\Phi_F = 0.11$. When the emission spectral data were mapped onto chromaticity coordinates on a Commission Internationale de l'Éclairage (CIE) 1931 colour space chromaticity diagram, we obtained values of (0.30, 0.36) for the (x, y) coordinates.

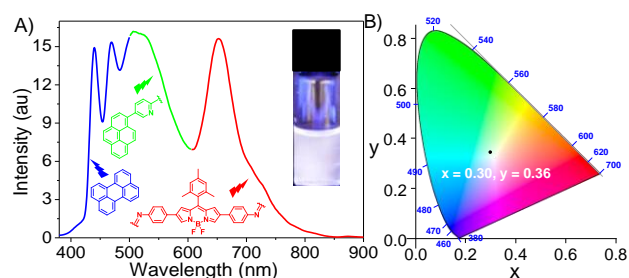


Fig. 4. (A) Fluorescence spectrum with photograph and (B) the CIE coordinates for a mixture of **5** (110 nM) and perylene (330 nM) in acetonitrile. $\lambda_{ex} = 365$ nm.

The cage architecture and the changes in its fluorescence upon interacting with perylene were critical in generating pure white light. Pyrene moiety in cage **5** contributes towards the green region of the spectrum whereas the BODIPY moiety in (guest-free) cage **5** has a minor contribution in the red region. Perylene adds the blue emission and importantly enhances the emission intensity of the BODIPY moieties in the red region thereby enabling white emission. The enhancement in the fluorescence of the BODIPY moiety in the presence of perylene could be attributed to excitation energy transfer from perylene to BODIPY.⁷⁰ The importance of cage and the bound perylene for white light emission was further exemplified in a control experiment wherein the fluorescence from a mixture of **1**, **2** and perylene has been recorded (Fig. S20). This solution exhibited fluorescence in the blue and green regions and the corresponding (x, y) coordinates on the CIE diagram were found to be (0.24, 0.33). This solution, however, lacked emission in the red region which can only be generated from the perylene-bound cage. Thus, by combining the photophysical and guest-binding properties of cage **5**, we have developed a new strategy for tuning colour of light emission.

Assignment of the mechanism of interaction between **5** and PAHs is challenging, due to the significantly lower perturbations to the host's absorption and emission spectra in the presence of these prospective guests. As the addition of perylene to **5** resulted in negligible changes in the fluorescence from pyrene and a moderate enhancement in the emission intensity from BODIPY, we assume that perylene could be selectively interacting with the BODIPY moieties of **5**. The driving force for the interaction between **5** and perylene is inferred to be the π - π stacking between perylene and BODIPY. As such stacking interactions are known to be weaker in non-aqueous solvents,⁶⁶ the smaller variations in the absorption and emission spectra upon the addition of perylene are not unexpected. Furthermore, neutral perylene (as compared to the

negatively charged anions) is expected to bind weakly to the positively-charged cages.

Self-destructive Amino Acid Recognition

Reaction-based chemical indicators are systems wherein substrate-triggered reactions are used to signal the presence of a given analyte.⁷¹⁻⁷³ In general, the reaction of the indicator with the analyte results in a structural change that leads to measurable changes in the optical properties of the indicator.⁷⁴⁻⁷⁶ Previous reports indicate that supramolecular assemblies can undergo subcomponent exchange with added aldehydes or amines.⁷⁷⁻⁷⁹ The feasibility of such exchange processes was found to be dependent on the relative reactivities of the subcomponents in question. Therefore, we anticipated that the reaction of M_4L_6 cages with suitable amines would liberate the bis(aminophenyl)BODIPY **1**, which could serve as a signalling event for amine detection.

In order to verify this hypothesis, we studied the interaction of **4** with selected amino acids. Thus, titration of cysteine into a solution of **4** resulted in a regular decrease in the absorbance at 555 nm along with the emergence of a broad peak in the region between 625-725 nm with an isosbestic point at 606 nm (Fig. 5). Similarly, the fluorescence spectrum of **4** exhibited an initial enhancement in intensity with the addition of cysteine. On standing for *ca.* 5 hours, the absorption spectrum of a mixture of **4** and cysteine resembled that of the free subcomponent **1** and the fluorescence of the solution had been completely quenched. The corresponding changes in the fluorescence titration data of **4** with other amino acids are shown in Fig. S21. Different amino acids interacted with **4** in a similar fashion to cysteine, but with varying rates of reaction. These absorption and fluorescence titration data are consistent with the reaction of amino acids with **4** leading to the release of **1**.

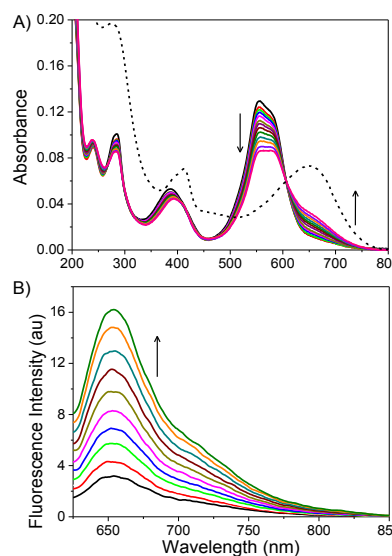
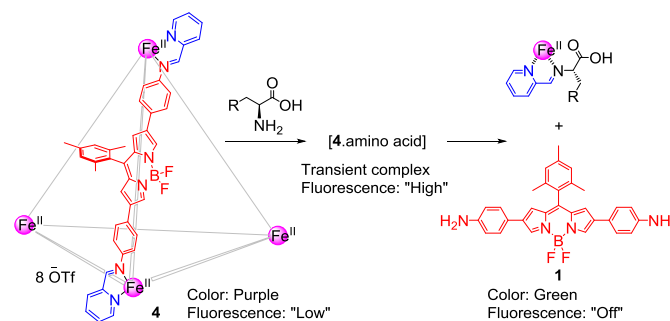


Fig. 5. Changes in the (A) absorption and (B) fluorescence spectra of **4** (52 nM) with the addition of cysteine (0-161 μ M) in 50% acetonitrile-water mixture. λ_{exc} = 610 nm. Dashed trace in (A) shows the absorption spectrum of the mixture after 5 hours.

On the basis of these data, we infer that the addition of an amino acid to a solution of **4** initially resulted in a transient complex [4.amino acid] having higher fluorescence as compared to the cage. This event was followed by the substitution of the BODIPY-based imines to generate amino acid-centered imines, leading to the formation of the corresponding amino-acid-based mononuclear complexes (Scheme 3). Simultaneously, bis(aminophenyl)BODIPY **1** was released, which accounts for the red-shift in absorption and loss of fluorescence. ¹H NMR titrations provided further evidence in support of this mechanism (Fig. 6). The addition of 2 equivalents of cysteine to a solution of **4** resulted in peaks corresponding to free 2-formylpyridine, which indicates the dissociation of the cage. Subsequently, when the concentration of amino acid was in large excess relative to that of the cage, we observed a NMR spectrum consistent with that of the free subcomponent **1** along with the formation of an insoluble precipitate. We infer the precipitate to contain the mononuclear Fe^{II} complex formed from cysteine and 2-formylpyridine. This experiment thus exploits the dynamic nature of the cages' imine bonds for detecting amino acids through a reaction based indicator approach, wherein the imines in **4** were transformed into the linear bisamine **1** by reaction with amino acids. The accompanying colour changes served to signal the analyte's presence.



Scheme 3. Schematic representation of amino acid recognition by **4**.

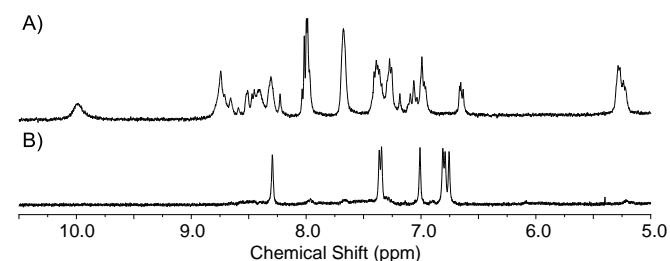


Fig. 6. Partial ¹H NMR spectra of cage **4** following the addition of (A) **2** and (B) 100 equivalents of cysteine in 50% CD₃CN-D₂O mixture.

Table 1. Guest Binding Properties of Cage 4

Guest	Mode of Interaction	Binding Affinity	Colour Change	Fluorescence change
Anions	Encapsulation	High	Purple to blue	Strong enhancement
Polycyclic aromatic hydrocarbons	Encapsulation	Low	-	Weak enhancement
Amino acids	Reaction	-	Purple to green	Completely quenched

Conclusions

We have synthesized a series of fluorescent metallo-supramolecular cages by incorporating BODIPY and pyrene fluorophores. Individual subcomponents exhibited useful optical spectroscopic properties that underwent well-defined changes upon cage formation. Investigation of the guest binding properties of these cages, as noted in Table 1 for the most versatile exemplar, cage 4, indicated that they (i) were capable of reporting on nanomolar concentrations of anions, which led to the development of a test-paper strip assay for the visual detection of anions; (ii) could form a white light emitting ensemble with perylene; and (iii) functioned as reaction-based indicator for the visual recognition of amino acids. The novelty of the systems presented herein is that metallo-supramolecular cages synthesized from the same building blocks are capable of performing multiple functions. These systems thus provide a foundation upon which future practical applications can be built, such as new chemoselective sensors, through the immobilization of such cages on polymer substrates.

Acknowledgements

This research was funded by the European Research Council. We thank the NMR service team at the Department of Chemistry, University of Cambridge for help with NMR, the EPSRC Mass Spectrometry Service at Swansea for providing Mass Spectra, and Veerasak Srisuknimit for having undertaken preliminary studies on a related BODIPY system.

Notes and references

^a Department of Chemistry, University of Cambridge Lensfield Road, Cambridge CB2 1EW (UK). E-mail: jrn34@cam.ac.uk

† Electronic Supplementary Information (ESI) available: Experimental procedures, synthesis and characterization data for subcomponents and cages, and optical and NMR titration data. See DOI: 10.1039/b000000x/

- M. L. Saha, S. De, S. Pramanik and M. Schmittel, *Chem. Soc. Rev.*, 2013, **42**, 6860-6909.
- S. Lee, C.-H. Chen and A. H. Flood, *Nat. Chem.*, 2013, **5**, 704-710.
- G. L. Fiore, S. J. Rowan and C. Weder, *Chem. Soc. Rev.*, 2013, **42**, 7278-7288.
- J. E. Beves, C. J. Campbell, D. A. Leigh and R. G. Pritchard, *Angew. Chem. Int. Ed.*, 2013, **52**, 6464-6467.
- M.-K. Chung, P. S. White, S. J. Lee, M. L. Waters and M. R. Gagné, *J. Am. Chem. Soc.*, 2012, **134**, 11415-11429.
- M. Albrecht and E. Hahn, *Top. Curr. Chem.*, Springer, Berlin Heidelberg, 2012.
- B. Rybtchinski, *ACS Nano*, 2011, **5**, 6791-6818.
- R. S. Forgan, J.-P. Sauvage and J. F. Stoddart, *Chem. Rev.*, 2011, **111**, 5434-5464.
- M. Mastalerz, *Angew. Chem. Int. Ed.*, 2010, **49**, 5042-5053.
- B. Icli, E. Sheepwash, T. Riis-Johannessen, K. Schenk, Y. Filinchuk, R. Scopelliti and K. Severin, *Chem. Sci.*, 2011, **2**, 1719-1721.
- P. D. Frischmann and M. J. MacLachlan, *Chem. Soc. Rev.*, 2013, **42**, 871-890.
- M. G. Cowan and S. Brooker, *Coord. Chem. Rev.*, 2012, **256**, 2944-2971.
- Y. Inokuma, M. Kawano and M. Fujita, *Nat. Chem.*, 2011, **3**, 349-358.
- R. Chakrabarty, P. S. Mukherjee and P. J. Stang, *Chem. Rev.*, 2011, **111**, 6810-6918.
- K. Mahata and M. Schmittel, *J. Am. Chem. Soc.*, 2009, **131**, 16544-16554.
- I. S. Tidmarsh, T. B. Faust, H. Adams, L. P. Harding, L. Russo, W. Clegg and M. D. Ward, *J. Am. Chem. Soc.*, 2008, **130**, 15167-15175.
- K. Harano, S. Hiraoka and M. Shionoya, *J. Am. Chem. Soc.*, 2007, **129**, 5300-5301.
- T. K. Ronson, S. Zarra, S. P. Black and J. R. Nitschke, *Chem. Commun.*, 2013, **49**, 2476-2490.
- H. Bunzen, Nonappa, E. Kalenius, S. Hietala and E. Kolehmainen, *Chem. Eur. J.*, 2013, **19**, 12978-12981.
- X.-P. Zhou, J. Liu, S.-Z. Zhan, J.-R. Yang, D. Li, K.-M. Ng, R. W.-Y. Sun and C.-M. Che, *J. Am. Chem. Soc.*, 2012, **134**, 8042-8045.
- S. Yi, V. Brega, B. Captain and A. E. Kaifer, *Chem. Commun.*, 2012, **48**, 10295-10297.
- M. M. J. Smulders, I. A. Riddell, C. Browne and J. R. Nitschke, *Chem. Soc. Rev.*, 2013, **42**, 1728-1754.
- H. Takezawa, T. Murase and M. Fujita, *J. Am. Chem. Soc.*, 2012, **134**, 17420-17423.
- P. Mal, B. Breiner, K. Rissanen and J. R. Nitschke, *Science*, 2009, **324**, 1697-1699.
- Z. J. Wang, K. N. Clary, R. G. Bergman, K. N. Raymond and F. D. Toste, *Nat. Chem.*, 2013, **5**, 100-103.
- D. Samanta and P. S. Mukherjee, *Chem. Commun.*, 2013, **49**, 4307-4309.
- R. Gramage-Doria and J. N. H. Reek, *ChemCatChem*, 2013, **5**, 677-679.
- C. He, J. Wang, L. Zhao, T. Liu, J. Zhang and C. Duan, *Chem. Commun.*, 2013, **49**, 627-629.
- M. Han, R. Michel, B. He, Y.-S. Chen, D. Stalke, M. John and G. H. Clever, *Angew. Chem. Int. Ed.*, 2013, **52**, 1319-1323.
- V. Ramamurthy and A. Parthasarathy, *Isr. J. Chem.*, 2011, **51**, 817-829.
- C. Schouwey, R. Scopelliti and K. Severin, *Chem. Eur. J.*, 2013, **19**, 6274-6281.

32. K. Mahata, P. D. Frischmann and F. Würthner, *J. Am. Chem. Soc.*, 2013, **135**, 15656-15661.
33. L. Fabbrizzi and A. Poggi, *Chem. Soc. Rev.*, 2013, **42**, 1681-1699.
34. R. Custelcean, P. V. Bonnesen, N. C. Duncan, X. Zhang, L. A. Watson, G. Van Berkel, W. B. Parson and B. P. Hay, *J. Am. Chem. Soc.*, 2012, **134**, 8525-8534.
35. Z. Laughrey and B. C. Gibb, *Chem. Soc. Rev.*, 2011, **40**, 363-386.
36. S. Kubik, *Chem. Soc. Rev.*, 2010, **39**, 3648-3663.
37. N. Kishi, Z. Li, Y. Sei, M. Akita, K. Yoza, J. S. Siegel and M. Yoshizawa, *Chem. Eur. J.*, 2013, **19**, 6313-6320.
38. B. K. McMahon and T. Gunnlaugsson, *J. Am. Chem. Soc.*, 2012, **134**, 10725-10728.
39. Z. Li, N. Kishi, K. Yoza, M. Akita and M. Yoshizawa, *Chem. Eur. J.*, 2012, **18**, 8358-8365.
40. O. Chepelin, J. Ujma, X. Wu, A. M. Z. Slawin, M. B. Pitak, S. J. Coles, J. Michel, A. C. Jones, P. E. Barran and P. J. Lusby, *J. Am. Chem. Soc.*, 2012, **134**, 19334-19337.
41. A. M. Johnson, O. Moshe, A. S. Gamboa, B. W. Langloss, J. F. K. Limtiaco, C. K. Larive and R. J. Hooley, *Inorg. Chem.*, 2011, **50**, 9430-9442.
42. Y. Liu, X. Wu, C. He, Z. Li and C. Duan, *Dalton Trans.*, 2010, **39**, 7727-7732.
43. J. R. Hiscock, C. Caltagirone, M. E. Light, M. B. Hursthouse and P. A. Gale, *Org. Biomol. Chem.*, 2009, **7**, 1781-1783.
44. A. E. Hargrove, S. Nieto, T. Zhang, J. L. Sessler and E. V. Anslyn, *Chem. Rev.*, 2011, **111**, 6603-6782.
45. B. W. Tresca, L. N. Zakharov, C. N. Carroll, D. W. Johnson and M. M. Haley, *Chem. Commun.*, 2013, **49**, 7240-7242.
46. A. Suzuki, K. Kondo, M. Akita and M. Yoshizawa, *Angew. Chem. Int. Ed.*, 2013, **52**, 8120-8123.
47. F. Zapata, A. Caballero, N. G. White, T. D. W. Claridge, P. J. Costa, V. t. Félix and P. D. Beer, *J. Am. Chem. Soc.*, 2012, **134**, 11533-11541.
48. N. Boens, V. Leen and W. Dehaen, *Chem. Soc. Rev.*, 2012, **41**, 1130-1172.
49. M. A. H. Alamiry, J. P. Hagon, A. Harriman, T. Bura and R. Ziessel, *Chem. Sci.*, 2012, **3**, 1041-1048.
50. A. Loudet and K. Burgess, *Chem. Rev.*, 2007, **107**, 4891-4932.
51. H. L. Kee, C. Kirmaier, L. Yu, P. Thamyongkit, W. J. Youngblood, M. E. Calder, L. Ramos, B. C. Noll, D. F. Bocian, W. R. Scheidt, R. R. Birge, J. S. Lindsey and D. Holten, *J. Phys. Chem. B*, 2005, **109**, 20433-20443.
52. Y. Hayashi, S. Yamaguchi, W. Y. Cha, D. Kim and H. Shinokubo, *Org. Lett.*, 2011, **13**, 2992-2995.
53. A. Martin, C. Long, R. J. Forster and T. E. Keyes, *Chem. Commun.*, 2012, **48**, 5617-5619.
54. A. M. Swinnen, M. Van der Auweraer, F. C. De Schryver, K. Nakatani, T. Okada and N. Mataga, *J. Am. Chem. Soc.*, 1987, **109**, 321-330.
55. M. C. Young, A. M. Johnson, A. S. Gamboa and R. J. Hooley, *Chem. Commun.*, 2013, **49**, 1627-1629.
56. W. Meng, J. K. Clegg, J. D. Thoburn and J. R. Nitschke, *J. Am. Chem. Soc.*, 2011, **133**, 13652-13660.
57. R. W. Saalfrank, H. Maid and A. Scheurer, *Angew. Chem. Int. Ed.*, 2008, **47**, 8794-8824.
58. Molecular modelling was done at the MM2 level using CAChe Workspace, WorkSystem Pro Version 7.5.0.85
59. J. K. Clegg, J. Cremers, A. J. Hogben, B. Breiner, M. M. J. Smulders, J. D. Thoburn and J. R. Nitschke, *Chem. Sci.*, 2013, **4**, 68-76.
60. We observed similar colour changes in the presence of an aqueous solution of acetate as well, but included the results with azide in Fig. 3 because of the potential importance of detecting a toxic chemical.
61. A. Frontera, *Coord. Chem. Rev.*, 2013, **257**, 1716-1727.
62. H. T. Chifotides and K. R. Dunbar, *Acc. Chem. Res.*, 2013, **46**, 894-906.
63. M. M. Watt, M. S. Collins and D. W. Johnson, *Acc. Chem. Res.*, 2012, **46**, 955-966.
64. A. Vargas Jentzsch, D. Emery, J. Mareda, P. Metrangolo, G. Resnati and S. Matile, *Angew. Chem. Int. Ed.*, 2011, **50**, 11675-11678.
65. L. M. Salonen, M. Ellermann and F. Diederich, *Angew. Chem. Int. Ed.*, 2011, **50**, 4808-4842.
66. H.-J. Schneider, *Angew. Chem. Int. Ed.*, 2009, **48**, 3924-3977.
67. C. A. Hunter, *Angew. Chem. Int. Ed.*, 2004, **43**, 5310-5324.
68. M. R. Wasielewski, *Acc. Chem. Res.*, 2009, **42**, 1910-1921.
69. A. Sautter, B. K. Kaletaş, D. G. Schmid, R. Dobrawa, M. Zimine, G. Jung, I. H. M. van Stokkum, L. De Cola, R. M. Williams and F. Würthner, *J. Am. Chem. Soc.*, 2005, **127**, 6719-6729.
70. We have not attempted to quantify the energy transfer process because of the complications arising from the overlapped absorption and emission spectra of the three chromophores (perylene, pyrene and BODIPY).
71. J. Chan, S. C. Dodani and C. J. Chang, *Nat. Chem.*, 2012, **4**, 973-984.
72. L. You, J. S. Berman and E. V. Anslyn, *Nat. Chem.*, 2011, **3**, 943-948.
73. D.-G. Cho and J. L. Sessler, *Chem. Soc. Rev.*, 2009, **38**, 1647-1662.
74. T. F. Robbins, H. Qian, X. Su, R. P. Hughes and I. Arahamian, *Org. Lett.*, 2013, **15**, 2386-2389.
75. J. Jo, A. Olasz, C.-H. Chen and D. Lee, *J. Am. Chem. Soc.*, 2013, **135**, 3620-3632.
76. S.-W. Zhang and T. M. Swager, *J. Am. Chem. Soc.*, 2003, **125**, 3420-3421.
77. M. L. Pellizzaro, K. A. Houton and A. J. Wilson, *Chem. Sci.*, 2013, **4**, 1825-1829.
78. M. M. J. Smulders, A. Jimenez and J. R. Nitschke, *Angew. Chem. Int. Ed.*, 2012, **51**, 6681-6685.
79. A. Granzhan, C. Schouwey, T. Riis-Johannessen, R. Scopelliti and K. Severin, *J. Am. Chem. Soc.*, 2011, **133**, 7106-7115.